

Facies characteristics and depositional environments of Quaternary tufa deposits, Antalya, SW Turkey

Erdal Koşun

Accepted: 13 May 2012 / Published online: 17 June 2012
© Springer-Verlag 2012

Abstract This study describes the facies characteristics and the origin of widespread tufa deposits in Antalya Quaternary Basin in southwestern Turkey. The tufa formation covers an area of 630 km² and is up to 280 m thick. Its generation is related to three major terrace systems that developed during the Quaternary. The upper (240–315 m) and the middle terraces (sloping seaward from 40 to 150 m) are exposed above sea level, while the lower terrace is below sea level (–100 to –50 m). The Antalya tufas are classified into ten facies according to the lithological and petrographic characteristics as phytoherm framestone (Pf), boundstone a-phytoherm boundstone (Pb), b-stromatolitic-like tufa (SI), bedded micritic tufa (M), phytoclastic (Pc), oncoidal tufa (O), intraclastic tufa (I), microdetrital tufa (Md), palaeosols (Ps), pisolithic tufa a-channel type (P), b-pool type (Pp) and intraformational tufa conglomerate (Ic). Process oriented facies analyses, scanning electron microscopy (SEM) and isotopic studies indicate fluvial, marsh, lacustrine and waterfall/cascade depositional environments, all formed through biological and physicochemical effects under cool (ambient) water conditions. Stable isotopic data ($\delta^{18}\text{O}$, $\delta^{13}\text{C}$) of Antalya Tufa is indicative of cold-water conditions, which are affected by seasonal temperature changes. The ²³⁰Th/²³⁴U ages obtained from the lower parts of the middle terrace indicate that the deposition started at least prior to 380 ka. On the other hand, ¹⁴C ages (16.85 and 3.56 ka) obtained from the upper parts of the middle terrace indicate that the deposition lasted till at least 3.56 ka. The upper terrace tufa deposition occurred during Early-Mid Quaternary by

tectonic uplift. Following the deposition, the first escarpment was probably formed in Mid Quaternary. Lower and middle terrace depositions are both controlled by eustatic sea level changes and tectonic uplift that occurred during Mid-Late Quaternary. The formation of the second escarpment at the lower terrace (Latest Pleistocene-Holocene) by glacio-eustatic sea level rise is followed by the formation of the third escarpment in the middle terrace (Holocene to Recent) by tectonic uplift and coastal cliff erosion.

Keywords Tufa terraces · Cool water · Stable isotopes · Terrestrial environments · Antalya · SW Turkey

Introduction

Travertine and tufa are carbonate rocks that precipitate in freshwater environments (Ford and Pedley 1996; Janssen et al. 1999; Pedley 2009). These terms are generally used alternatively although both describe different formations, especially from the viewpoint of depositional conditions (Pedley 1990; Ford and Pedley 1996; Carthew et al. 2006). Pentecost (2005) reported that these freshwater calcium carbonate deposits were divided into two main groups as thermogene (formed under hot water conditions) and meteogene (formed under cool water conditions) depending on depositional conditions. Many authors agree that travertines are precipitated under hot water conditions (Chafetz and Lawrence 1994; Altunel 1996; Guo and Riding 1998; Fouke et al. 2000; Özkul et al. 2003). The travertines are often hard and crystalline rocks and frequently contain laminations and shrub-like bacterial growths (e.g. Guo and Riding 1998). However, tufa is mostly precipitated as physicochemical calcification

E. Koşun (✉)
Department of Geological Engineering,
Akdeniz University, 07200 Antalya, Turkey
e-mail: kosun@akdeniz.edu.tr

around stems of chara and vascular plants under cool (ambient) water conditions and typically contains the remains of micro and macrophytes animal and bacteria (Pedley 1990; Ford and Pedley 1996; Guo and Riding 1998; Janssen et al. 1999), and also has a porous structure.

The aim of this study is to provide a new approach to the definition of tufa formations encountered in Antalya region and to make a detailed classification and characteristics of the depositional features of the Antalya Tufa. In addition to seven facies, already described by Pedley (1990) and Glover and Robertson (2003), two additional facies are described for the first time in this study within the Antalya Tufa namely very extensive bedded micritic tufa and channel type pisolitic tufa (pisolitic tufa: pool type and channel type). In addition, the phytoherm boundstone tufa facies described by Glover and Robertson (2003) is re-interpreted as boundstone facies and divided into two sub-facies as phytoherm boundstone and stromatolite-like tufa. Moreover, the stable isotope studies are used to provide some additional information on the environmental conditions of tufa formations.

Geological and geomorphological setting of the Antalya Tufa

Studies on Antalya Tufa (AT) have been conducted by the many researchers (e.g. Planhol 1956; Vita-Finzi 1969; Burger 1990; Ford and Pedley 1996; Glover and Robertson 2003) and the majority (e.g. Planhol 1956; Burger 1990) described these freshwater carbonate rocks as travertine. The term tufa was first used by Ford and Pedley (1996). Travertines are mostly described as laminated carbonate precipitations that are formed by inorganic–organic processes of hydrothermal originated fresh waters in high temperatures at the terrestrial environments. They are generally free of macrophyte and animal remnants. On the contrary, tufas are porous terrestrial carbonate precipitations, which are formed in cold-water conditions and typically contain micro/macro-scaled plant, animal remnants and products of bacterial activity (Ford and Pedley 1996; Janssen et al. 1999). The carbonate rocks of Antalya region clearly contain macrophyte, animal remnants and bacterial activity, represent cold-water conditions and are evaluated as tufa in this study.

The AT is located in the central part of Antalya Quaternary basin of southwest Turkey and is the most extensive tufa depositional area in the world. It covers a surface area of approximately 630 km² and is about 280 m thick (Burger 1990; Özüş 1992; Pentecost 2005). The AT crops out within the Antalya city borders between 36°50′–37°10′ north latitude and 30°32′–30°52′ east longitude (Fig. 1a). The tufa basin is surrounded by Beydağları Mountains to

the west-northwest, Aksu River to the east and the Mediterranean Sea to the south (Fig. 1a). The tufas become thinner towards the east and west. In the east, they overly the Pliocene Alakilise Formation of the Aksu Basin as a thin cover (Çiner et al. 2008). In the west, they become thinner towards the Mesozoic carbonates of the Beydağları Mountains (Fig. 1b). Recent alluvial fans in the study area consist of unconsolidated hillside colluviums and are composed of pebbles, sand and mud accumulated on mountain slopes. Active beaches in the southern part of the area are mainly made up of pebbles (derived from Mesozoic carbonates and ophiolitic rocks) and coarse sand. Local coastal dunes, 1–3 m wide and up to 1 m high, are developed in the southeastern seashore. Major fluvial systems, which are also responsible for the continuing tufa deposition, mainly extend in the study area on a north–south axis.

The AT is formed by three step-like terraces with a flat topography (Fig. 1b, c). These are the upper terrace (Fig. 2a, b), the middle terrace (Fig. 2c, d) and the lower terrace under the sea level. According to subsurface data, the tufa has a thickness of 99–245 m in the upper terrace and 65–85 m in the middle terrace (Özüş 1992). These two terrace systems meet in the northeastern part, where the total tufa thickness decreases down to 20–30 m. Geophysical data (Burger 1990; Özüş 1992) indicate the existence of a wide terrace, up to 50–100 m in thickness, below sea level. This lower terrace extends to the south almost 3 km from the recent seashore and continues down to a depth of 150 m. Burger (1990) and Glover and Robertson (2003) stated that the age of the AT ranges from >600 to 87 ka based on U/Th isotopic data. The main spring source for the AT deposition corresponds to the Kırkgöz Springs, which is situated in the northwestern edge of the upper terrace at 315 m above sea level. In addition, the Düden River flows over the middle terrace from a spring source near the upper terrace escarpment to the south. In the west, the Karaman Çay River has cut a deep gorge through both the upper and middle terraces, carrying clastic sediments to the sea. The modern spring waters are discharged from karstic aquifers with very large groundwater reservoirs from carbonate platforms, notably the Beydağları Mountains to the west of the Antalya Basin. Modern tufa deposition is minimal nowadays except very local occurrences at waterfalls inland and along the coastal areas (Fig. 2c). Very small quantities of carbonate encrusted aquatic plants can be found in the Kırkgöz Springs (Ekmekci 2005). A small amount of microcrystalline tufa is also observed to be precipitated in pools and gently flowing streams.

Besides the Antalya area, several travertine and tufa outcrops are also observed around Burdur–Bucak area to the north of the AT (Fig. 1). They are located essentially to the east of Bucak and Kocaaliler in the Aksu Basin

Fig. 1 continued

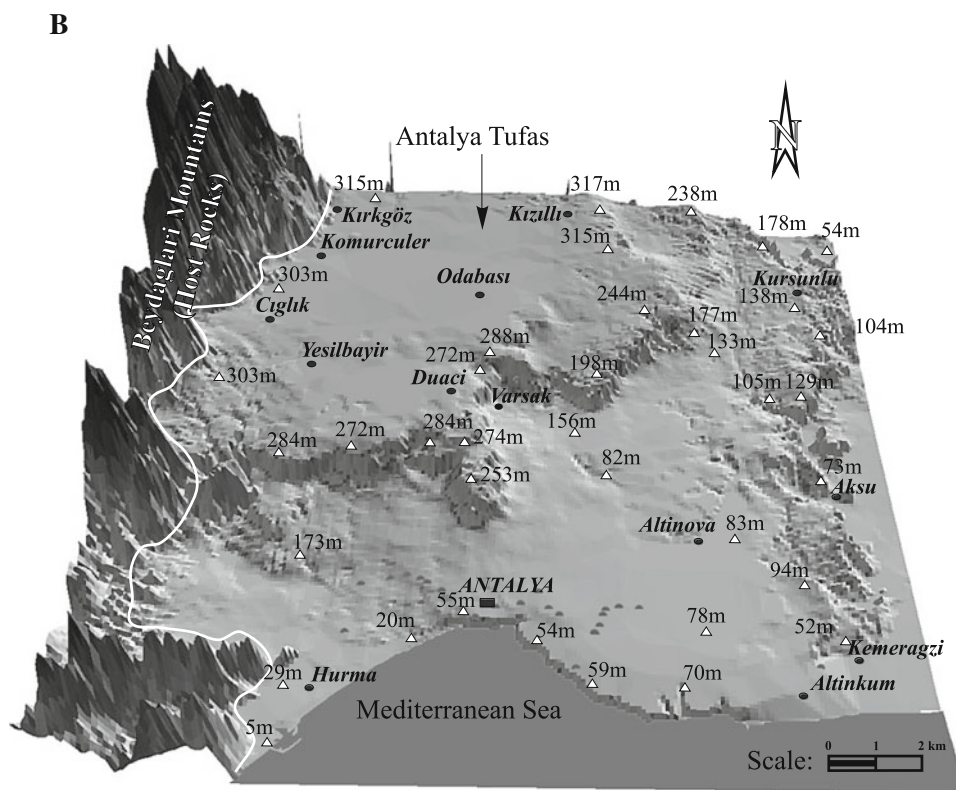


(Fig. 1). The outcrops located on the eastern side of the Aksu valley are Kocaaliler–Kargı: 700–900 m, Kızılseki: 500 m, Çamlık: 1,000–1,200 m and Taşayla: 800–1,000 m. On the western side of the valley Şenel (1997) reported an outcrop near Çandır. The Çukurköy outcrop (+1,500 m) is located to the north of the Aksu basin. In these areas, the travertine unconformably covers both the Antalya Nappes and the Miocene conglomerates (Fig. 1). Previously, Poisson et al. (2003), Flecker et al. (2005) and Çiner et al. (2008) have provided information on the stratigraphy of the Aksu Basin. From bottom to the top they described: (1) Kargı conglomerates and Karpuzçay marls (Serravallian–Tortonian), (2) Gebiz Limestone (Messinian), (3) Eskiköy Formation (Lower Pliocene), (4) Yenimahalle Formation (Lower Pliocene), and (5) Alakilise Formation. (Middle–Upper Pliocene), Antalya Tufa and Bucak Travertine (Plio–Quaternary).

Methods

Tufa lithotypes were mainly distinguished on the basis of field observations. In addition to the field features of tufa, hand specimens were collected especially from cliffs, roadcuts and foundations of buildings. A total of 164 samples, representing different lithotypes of tufa deposits, were collected to determine their sedimentological and petrographic features (Table 1). Additionally four samples (two

for C14 and two for $^{230}\text{Th}/^{234}\text{U}$ analyses) were also collected for age determination purposes (Table 1). $^{230}\text{Th}/^{234}\text{U}$ analyses were carried out in Paul Scherrer Institute, Switzerland. More than 120 tufa samples were prepared for thin section studies and examined by using a polarizing microscope. Eight samples were studied with scanning electron microscopy (SEM, Model: CAMECA SU 30, Mode: SE, Accelerating voltage: 15 kV) in Hacettepe University (Ankara). Eighteen rock samples were analyzed to determine $\delta^{18}\text{O}$ and $\delta^{13}\text{C}$ values. ^{14}C age studies were carried out from a lignite level of the upper-middle terrace and palaeosol of the uppermost part of the southern middle terrace. Diagenetic mineral formations, mineral transformations such as aragonite–calcite, primary and secondary mineral formations and processes (algae, bacteria, and cyanobacteria activities) have also been investigated.

Carbon and oxygen isotope composition of tufa samples were analyzed at the University of Tübingen using the orthophosphoric acid method of McCrea (1950). Isotopic ratios were measured on a Finnigan MAT 252 gas-mass spectrometer with a precision of ± 0.1 at the Geochemical Central Laboratories, University of Tübingen, Germany. Radioactive ^{14}C dating of tufa samples were analyzed in ^{14}C Laboratories of French Atomic Energy Commission (CEA) and University of Paris, Saclay, France by using scan accelerator mass spectrometry (SMA Artemis-LMC14).



Fig. 2 General view of Antalya Tufa (**a–b** upper terrace and **c–d** middle terrace; 40 m thick). **b** Close up view of the stromatolitic-like tufa facies. **c** Düden River (one of the major rivers responsible for the

actual tufa formation) waterfall into the Mediterranean Sea in the Lara area (east of Antalya town). Arrows in **a** indicate tufa terraces

Tufa lithotypes of the AT: macrofacies and microfacies

Sedimentological descriptions of the AT are carried out according to Pedley's (1990) classification. General facies descriptions are given in Table 2. Two new tufa facies of AT are first described as “bedded micritic tufa” and “channel type pisolitic tufa” in this study.

In the proposed depositional model of AT (Fig. 3), which precipitated in fluvial, paludal, lacustrine and waterfall-cascade environments, is classified into ten lithofacies related to lithological and petrographical diversity as follows; boundstone (a-phytoherm boundstone, b-stromatolitic-like tufa), phytoherm framestone, bedded micritic tufa, phytoclastic tufa, oncoidal tufa, intraclastic tufa, microdetrital tufa, palaeosols, pisolitic tufa (a-channel type and b-pool type) and intraformational tufa conglomerate.

In the AT, three autochthonous and seven allochthonous tufa facies are described as follows:

Autochthonous tufa deposits

Autochthonous tufa deposits of AT were divided into three facies as boundstone (a-phytoherm boundstone,

b-stromatolitic-like tufa), phytoherm framestone and bedded micritic tufa according to their lithologic, petrographic characteristics and depositional environment.

Boundstone

Description The boundstone facies has characteristic features of laminated and stromatolitic tufa deposits (e.g. Freydet and Verrecchia 1999; Fig. 4a). Laminated tufa deposits generally represent light and dark colour pairs or a varve-like pattern that display a bush-like growth formed by dense microcrystalline layers (Fig. 4b).

They have been previously described by Glover and Robertson (2003) as phytoherm boundstone deposits, which consist of horizontal, undulate and domal algal mats. However, in this study, this facies is divided into two different sub-facies according to their origin (biogenic or non-biogenic). The first sub-facies, a-phytoherm boundstone, has similar properties of Pedley (1990)'s “Phytoherm boundstone” facies and was formed on the middle terrace by biogenic activity. The second sub-facies, stromatolite-like tufa (non-biogenic), was formed on the upper terrace by changes in hydrological and geochemical conditions.

Table 1 GPS locations of the samples

Location	Sample number	Latitude (N)	Longitude (E)
1	1, 2, 3, 4, 5, 6	2°98'852"	40°85'112"
2	7, 8, 9, 10, 11, 12, TU-6	2°93'707"	40°84'726"
3	13, 14, 15, 16, 17, 18, 19	2°96'039"	40°85'792"
4	20, 21, 22, 23, 24, 25, 26, 27, 28, 29, 30, 31, 32, 33, 42, 43, 44, 45, 46	2°91'546"	40°85'390"
5	34, 35, 36, 37	3°00'108"	40°85'623"
6	38, 39, 40, 41	3°02'025"	40°89'427"
7	47, 48	2°90'730"	40°86'858"
8	49, 50, 51	2°90'367"	40°87'585"
9	52	2°98'928"	40°89'678"
10	53, 146, 147, 148, 149, 150, 151, 152, 153, 154	2°99'367"	40°85'321"
11	57, 58, 59, 60	2°91'506"	40°86'422"
12	61	2°90'100"	40°86'471"
13	62, 63	2°89'430"	40°86'446"
14	64, 65	2°88'500"	40°84'120"
15	66, 67, 68	2°98'386"	40°84'047"
16	69, 70	2°97'638"	40°82'424"
17	71, 72	2°96'640"	40°84'944"
18	77, 78, 79, 80, 81, 82A, 82B, 84, 85, 86, 87, 88, 90, 91, 92, 93, 94, 95, 96, 97	2°96'126"	40°84'807"
19	99, 100, 101, 102	2°95'462"	40°85'441"
20	103, 104, 105, 106, 107	2°94'451"	40°84'464"
21	108	3°09'779"	40°85'946"
22	109	3°09'800"	40°85'869"
23	110, 111	3°09'216"	40°83'639"
24	112, 113, C2	3°07'043"	40°82'634"
25	114, 115, 116, 117, 118, 119	2°96'513"	40°96'509"
26	120, 121, 122	2°96'525"	40°96'907"
27	123, 124, 125, 126, 127, 128, 130	2°90'062"	40°91'536"
28	131, 132	2°96'944"	41°08'105"
29	134, 135	2°98'720"	40°84'913"
30	136	2°92'269"	40°86'065"
31	137, 138	2°91'658"	40°86'453"
32	139, 140, 141, 142, 143, C1, TU-1	2°96'585"	40°97'023"
33	144, 145	3°06'004"	40°97'400"
34	155, 156, 157	2°94'478"	40°85'282"
35	158, 159, 160, 161, 162, 163, 164	2°97'000"	40°84'900"

The boundstone facies shows different characteristics in the middle and upper terraces of AT. In the middle terrace, it consists of pairs of hard, honeycomb-shaped, highly porous, light coloured laminae, formed by insect larvae (Fig. 4c) and fine consolidated, dark-coloured laminae,

constructed by algal activity such as *Schizothrix* sp. and *Rivularia* sp. (Freytet and Verrecchia 1999; Arenas et al. 2000). In the upper terrace, the deposits are brittle and unconsolidated. However, they are fragile and loose when hit with a hammer (Fig. 4d). Large parts of the boundstones on the upper terrace are made up of radial grown bunch of dendritic calcite crystals. These bunch groups are 5–10 cm thick and separated by a few mm thick micritic levels (Fig. 4e). On the upper terrace, stromatolitic mats form heads of 3–4 m in diameter. They are composed of asymmetrical heads and domal build-ups of 50–100 cm in height. Wavy beds, each a couple cm thick, can also form thick (2–3 m) deposits on gentle slopes (Fig. 4f).

Interpretation Laminations depending on differences in growth of biotic activity were controlled by seasonal factors (e.g. Janssen et al. 1999) and/or changes of hydrologic regime. Golubic (1991) clearly showed that these seasonal differences were related to the cyanobacteria activities. Loosely packed and highly porous light-coloured laminae indicate the summer periods, whereas more densely packed and dark-coloured laminae with low porosity represent winter periods (Freytet and Verrecchia 1999; Janssen et al. 1999). The microscopic studies revealed that the chironomid insect larval was housed in the holes of the light-coloured laminae of phytoherm boundstone (Fig. 5a). On the other hand, in the phytoherm boundstone the dark-coloured laminae are thought to be related to calcified films of dome-shaped algal structures, such as *Schizothrix* sp., which are associated with the precipitation of small anhedral calcite crystals leading to early cementation of phytoherm (Fig. 5b). Seasonality, in these facies, is stated by annual oviposition by chironomid flies at the beginning of each summer (Golubic 1991). The light- and dark-coloured laminae couples have a typical cyclic pattern. The upward growing and concave-up nature of the larval housings are clearly determined by using SEM (see Fig. 4c).

Jones et al. (2000) reported that dendritic type calcite crystals in carbonate rocks may have been sharp edges and zigzag structures, which were precipitated by biogenic or non-biogenic agents around hot or cold springs. In addition to these features, various sized holes having very fine laminations, related to microdome structures in micritic levels, show great similarity to microbial biofilms, which were characterized by desiccation-shrinkage and gas-releasing structures (Arp et al. 1998). However, some samples, taken from the Varsak region (representing the upper terrace), are evaluated as stromatolitic-like subfacies in this study and do not represent traces of the biogenic activity. They are radial “bladed” fan-shaped crystals with subhedral and euhedral terminations and subparallel to feathery orientations. In this case the radial “bladed” fan-shaped crystalline fabric would be formed as crystalline

Table 2 Facies types of Antalya Tufa

Facies type	Description	Depositional environment
Autochthonous deposits		
Boundstone		
a-Phytoherm boundstone	Laminated tufa, in situ, biogenic	Waterfall/cascade
b-Stromatolitic-like tufa	Stromatolitic tufa, in situ, non-biogenic	
Phytoherm framestone	Tufa facies which is formed by encrust plant material, in situ	Paludal/marsh
Bedded micritic tufa	Tufa facies consisting of fine crystalline, massive and highly consolidated carbonate minerals	Lake/lacustrine
Allochthonous deposits		
Phytoclastic tufa	Allochthonous tufa facies which consist of plant fragment cemented during or after transportation	In stream, fluvial and lake system
Oncoidal tufa	Cylindrical tubes surrounded by laminae, resembling to water pipe-like structure tufa facies	In the agitated pools environments
Intraclastic tufa	Plant fragment rich, unconsolidated, sand-silt size detrital tufa facies	Generally, around of the phytoherm framestone and in fluvial channels
Microdetrital tufa	Tufa facies consisting of fine, unconsolidated carbonate sediments	In lake and pool
Palaeosols	Organic materials and carbonate-rich, unconsolidated red mudstone	As overbank deposits in fluvial environments
Pisolitic		
a-Pool type	Tufa facies consisting of hard, spheroidal or subspheroidal, pearly- like balls accumulate in small terraces and pools on the gentle cascade slope or in the fluvial channels	Fluvial channels and pools
b-Channel type		
Intraformational tufa conglomerate	Tufa conglomerate consist of subrounded to rounded pebbles	In fluvial channels

crust (e.g. Sant'Anna et al. 2004). Conversely, in the middle terrace of the AT similar-fan shaped structures are rich in thin microbial covers and vertical-grown algae such as *Shizotrix* and *Rivularis* (Fig. 5b, c). Especially, *Rivularis* can be easily determined by the shape of radially growing filaments within the densely packed calcite cement. From these points of view, calcite bunches must have been formed both as organic and inorganic. Chemical precipitation was induced by upright direction to the side slope at high flow velocity periods of waters or by agitated, rapidly flowing water around springs (Gonzalez et al. 1992). At low flow velocity regime, micritic precipitations forming microbial films have also covered the fan-type bunches, constructed by vertical growth of non-biogenic calcite crystals. The biogenetic activity is more effective in the middle terrace, whereas non-biogenic activity is more efficient in the upper terrace of the AT. Therefore, the origin of the boundstones formation of the AT can be attributed to biogenic and non-biogenic processes all over.

Phytoherm framestone

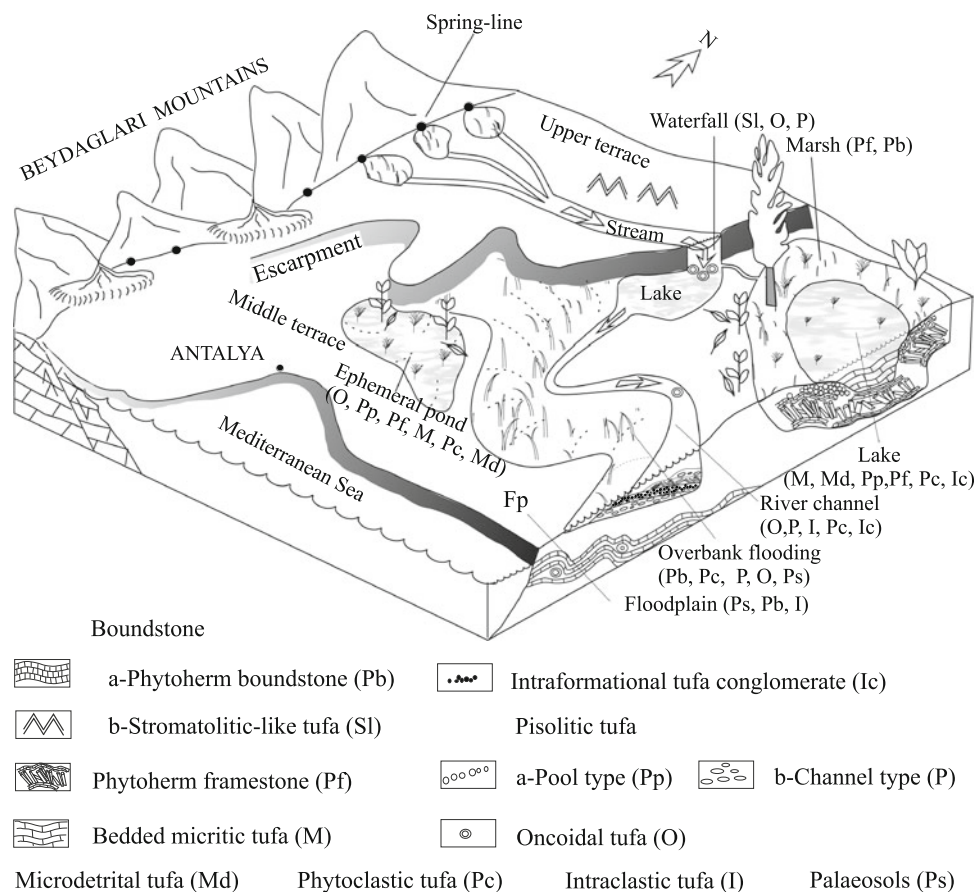
Description Phytoherm framestone facies is composed of calcified reeds, undefined plant branches, leaves and tree bodies (Fig. 5d). Morphologically they have a grain-

supported fabrics and exhibit great strength. The framework bearing macrophytic coatings have irregular orientations and complex structures, which are similar to the reef structures. The macrophytic coatings generally have laminations and consist of thick carbonate crusts up to 3–4 cm. Calcium carbonates have been cylindrically deposited around plant fragments as microbial (algae and cyanobacteria) material-rich micritic layers in general (Pedley 1990).

Plant bodies and branches, formed by phytoherm framework, were partly wiped out after being encrusted with carbonate (Arenas et al. 2000). They leave mould-like voids and are filled with coarse and blocky sparite in different portions. Some plant samples have also been calcified in a manner to preserve its woody tissue structure. Voids between calcified plant bodies included in situ growths that are filled by phytoclast and/or microdetrital clasts in different portions. In these cases, physical resistance of phytoherms increases providing its preservation. The length of these protected plants can exceeding 50 cm as observed in the field (see Fig. 5d).

Interpretation Phytoherm framestones generally occur as a result of the calcification of in situ macrophytes (e.g. woody plants, reeds, leaves, etc.). Many researchers have noted that calcium carbonate precipitation around plant

Fig. 3 Proposed depositional model for Antalya Tufa



bodies depended on microbial (algae and cyanobacteria) metabolic activities in phytoherm framestones (e.g. Pedley 1990; Arenas et al. 2000). Mainly tabular fragments, observed by SEM, have proved that microbial effects especially had been highly influential in forming micritic depositional textures within the Antalya phytoherm framestones (see Fig. 5e, f). This micritic formation, which is frequently a by-product of microbial metabolism, accumulates as surficial coatings on microbes and their extracellular polymeric substances (EPS) and sometimes within the EPS (e.g. Pedley 2009). In addition, microdetrital carbonates are also fixed on this surface. The microbial agent's depositions within the phytoherm framestone petrographically display the clotted shaped "thrombolytic" micrite lamination, where physicochemical calcite deposits especially occur as void fills, form coarse spar crystals and/or fringes (Fig. 6a).

Bedded micritic tufa

Description The micritic tufa facies is characterised by hard, fine crystalline, massive and highly consolidated units, 10–50 cm thick and 1–10 m wide, (Fig. 6b) and resemble the micritic limestones. It can be differentiated from chemical micritic limestones by the presence of plant

root voids, which intercalates with all sided-waterfall, pool and fluvial tufa deposits reflecting changes in lake level.

Interpretation Thin section studies clearly indicate the presence of plant root voids, ostracods and charophytic remains, indicating a low energy depositional environment like a lake and pool. The lower plant-bearing, massive, less porous bedded micritic tufa deposits are formed by deep lake processes. On the other hand, plant fragments are infrequent and more porous at shallow and lakeshore environments (Arenas et al. 2000). In that case, the facies vertically changes to phytoherm framestone (Fig. 6b). The bedded micritic tufa generally has no structure under the thin section but frequently is clotted and displays grumose texture (Pedley 1990). Millimetric holes within this facies were evaluated as traces of chara, ostracods and cyanobacteria filaments (Koşun et al. 2005). The lithological features of this facies clearly resemble the "biomicrite facies", previously described by Arenas et al. (2000), and indicate the deep-water palustrine and lacustrine environments.

Allochthonous tufa deposits

Allochthonous tufa deposits have been precipitated in their respective environments as a result of transportation

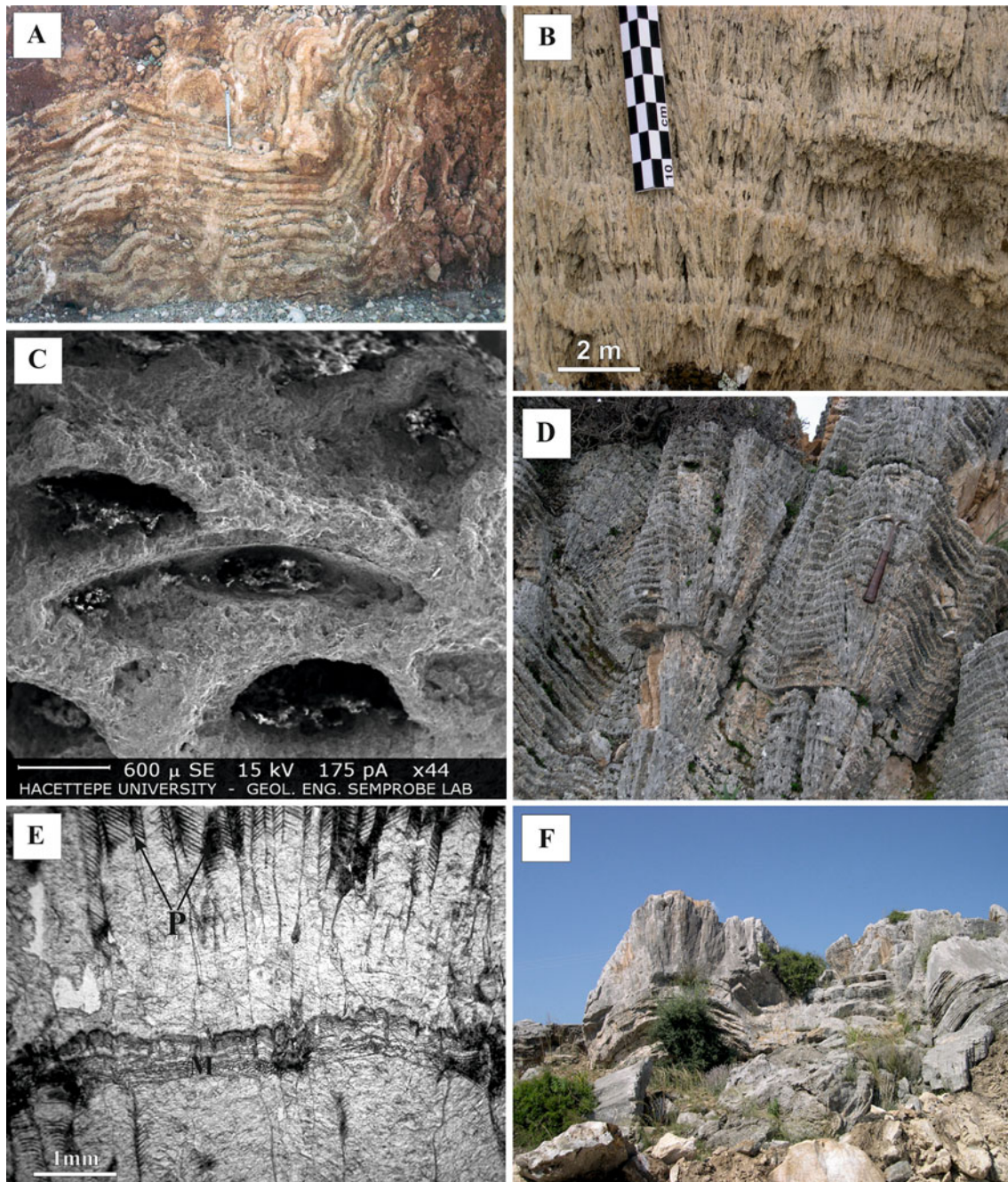


Fig. 4 Field views of **a** the vertical development of phytoherm boundstone facies, **b** stromatolitic-like tufa displaying bush-like growth formed from calcite crystals, **c** SEM view of light-colour laminae of phytoherm boundstone facies. Note the larval housings

processes. The fragments are derived from the anterior tufa facieses and can be classified according to the grain size, grain shape and petrographic features. Allochthonous tufa deposits of AT were divided into seven lithofacies as phytoclastic tufa, oncoidal tufa, pisolitic tufa, intraclastic tufa, microdetrital tufa, palaeosols, and intraformational tufa conglomerate according to their lithologic, petrographic characteristics and depositional environments.

showing upright growth (49), **d** and **f** general field views of stromatolitic-like tufa, **e** P: radial-fan shaped “palisadic-like” calcite crystals, which are constructed vertical-growth in stromatolitic-like tufa, M: micrite, 49: sample number

Phytoclastic tufa

Description The facies mainly consists of cement-encrusted and allochthonous plant fragments. They generally occur in situ or as re-deposition of weathered and transported phytoherm framestones. Detritals must be cemented during or after transportation. Precipitated leaves and branch fragments have a grain-supported

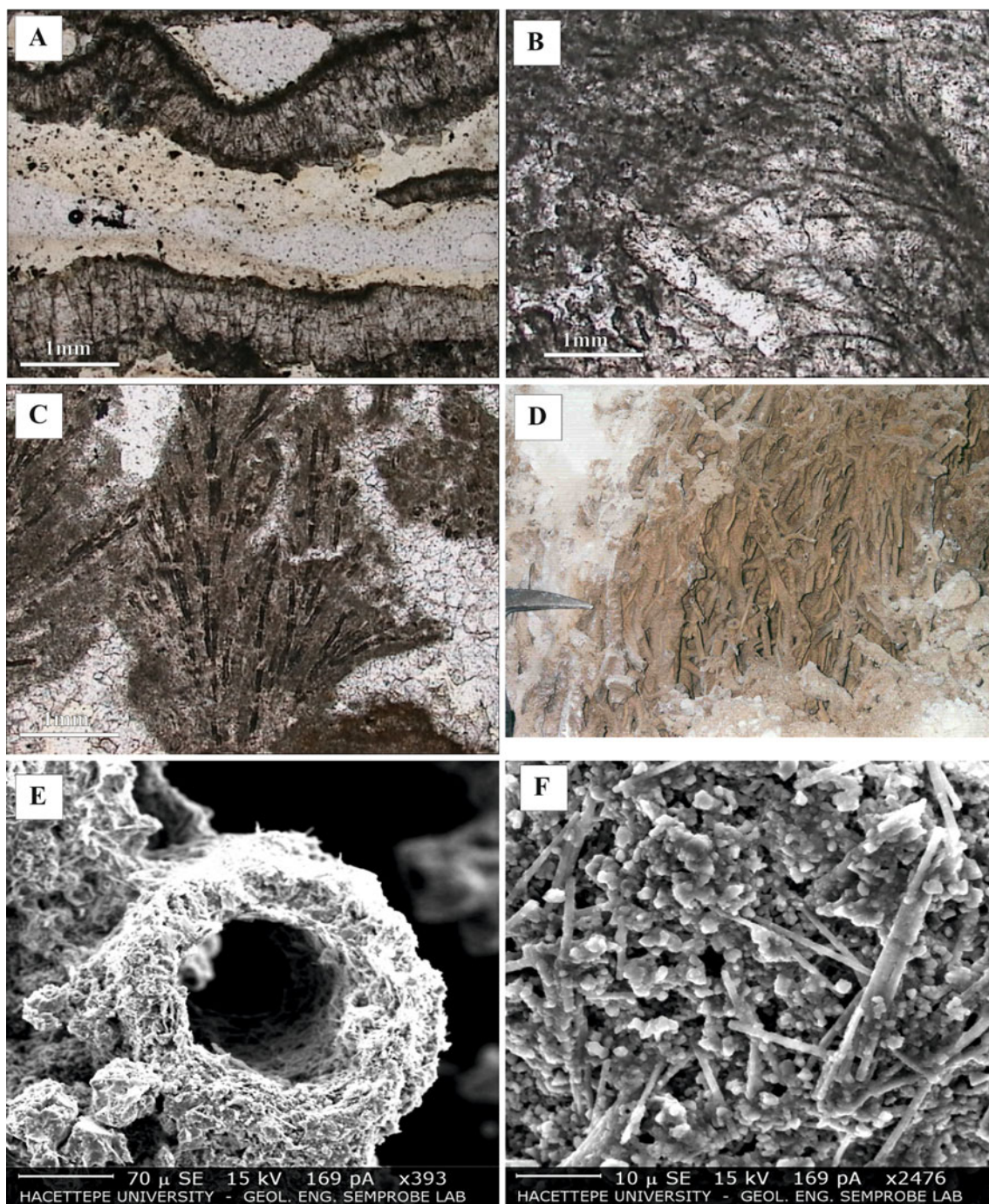


Fig. 5 Photomicrographs of **a** laminated “phytoherm boundstone” facies. Micrite laminae resulted from microbial precipitation and anhydrous calcite crystals (29), **b** *Schizothrix* sp. (29), **c** *Rivularis* sp. (39), **d** field view of phytoherm framestone formed by calcification of in situ growing plant. **e** SEM photomicrograph of phytoherm

framestone facies, which was formed by microbial filaments/agents. Grain-supported fabric and calcite minerals around plant moulds, deposited by microbial effects (111). **f** Close up view of **e** on SEM photomicrograph. Filaments and microspheroidal grains produced by calcified micro algae and microbial activity

fabric (Fig. 6c). Antalya deposits show cyclicity and locally individual units that can reach up to a few cm in thickness (Fig. 6d). They contain various scale cross-beddings, channels and gradation depending on flow velocity. The dragged branches and wood fragments

together with coarse gravel-sand size lithoclasts are common within the fluvial deposits. In fluvial-lake environments, the size of phytoclasts clearly becomes smaller and passes into intraclastic tufa facies (Fig. 6d). The depositional channels of the facies show continuity

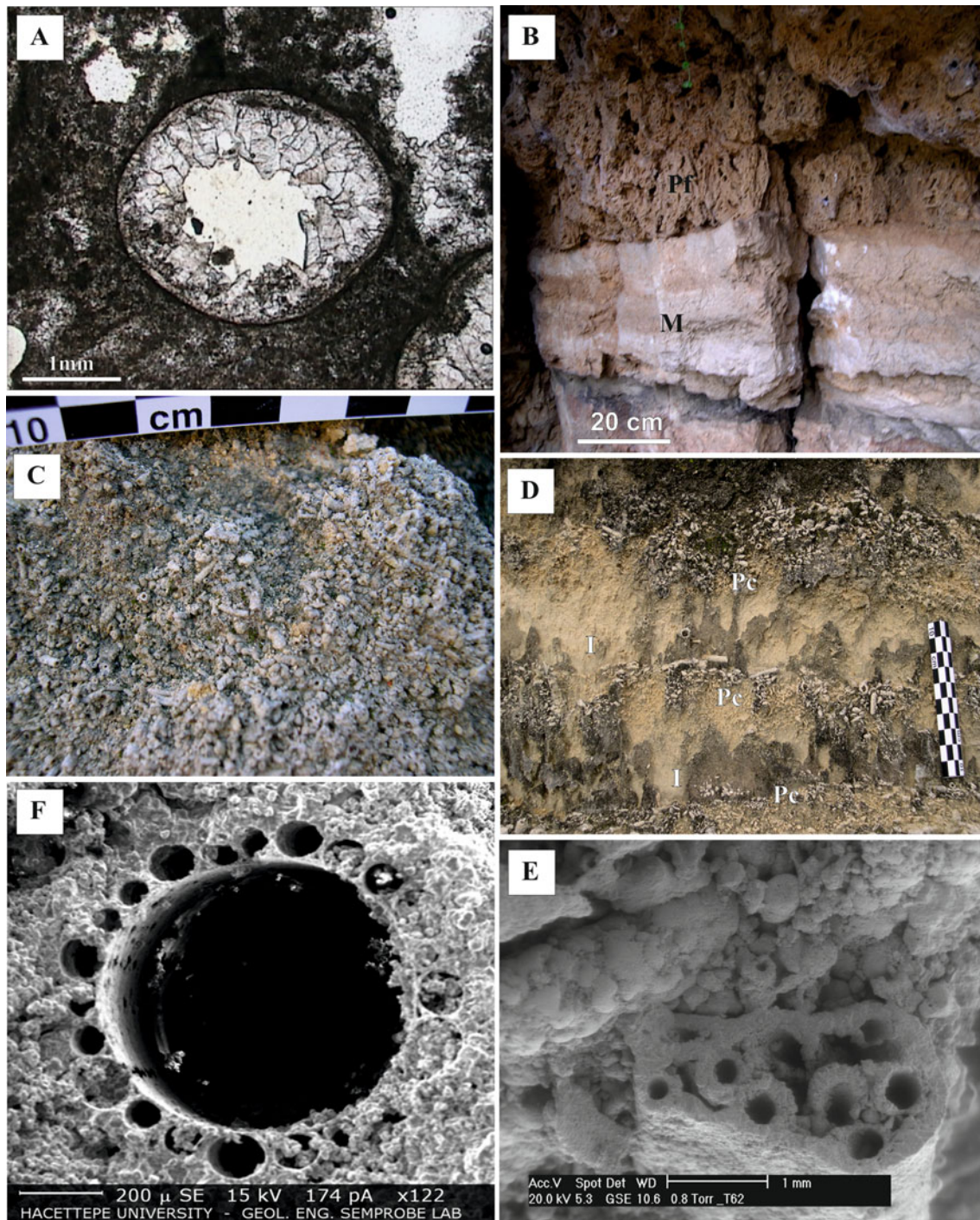


Fig. 6 **a** Microscopic view of phytotherm framestone, void-filling secondary calcite spars leading to early lithification of microbial structure during precipitation in vadose diagenesis (72). **b** Bedded micritic tufa and phytotherm framestone facies. M: bedded micritic tufa, Pf: phytotherm framestone. **c** Calcified plant fragments bearing phytoclastic tufa facies. **d** Alternations of intraclastic and phytoclastic layers in the Antalya Tufa, Pc Phytoclastic tufa, I Intraclastic tufa.

e SEM photomicrograph of plant fragments showing encrustation of the sheath by calcite; clot-like structure by microbial activity in the upper right corner of the picture. The heavy precipitation of the calcite on the sheaths may be due to CO₂ evasion and the resulting high degrees of super saturation of the water with respect to calcite along with photosynthetic carbonate (62). **f** SEM photomicrograph of calcified plant fragments (80)

from a few m to tens of m in length. Within the channels and along its sides, pisolites and oncolites facies are also observed within the facies.

Interpretation Phytoclastic tufa facies has been developed in fluvial and fluvial-lake systems (e.g. Pedley 1990). This facies, formed through disintegration of phytotherm

framestones, displays several features that resemble the phytoherm framestones under the microscope (Fig. 6e). However, voids from decaying plants are less common than in phytoherm framestones (Fig. 6f). These voids are often filled with secondary calcite spar (see Fig. 6a).

Oncoidal tufa

Description The facies is formed of oncoids, up to 0.2–10 cm in diameter, precipitated around plant fragments or a tree body nucleus, which are affected by biotic metabolism activity (Fig. 7a). They are differentiated from pisolite by means of an irregularly laminated cortex and larger diameter varying from 2 to 100 mm. The nuclei of these oncoids are either formed by branches, plant fragments or voids left behind by these materials. On the contrary, pisolites nuclei are exclusively formed by carbonate rock particles. In the investigated area they are generally found in phytoherm boundstones. They are cylindrical in shape and display a chimney or water pipe-like structures. More than one nucleus may be coalesced during the formation (Fig. 7a). Under the microscope bush-like structures, formed by colonized bacteria and algae, are also observed within coatings and the algal growth mostly at the end of calcified mucilaginous tubes (Fig. 7b), which helps to distinguish the biogenic and non-biogenic pisolites.

Interpretation These features indicate the agitated environments such as pools with waterfalls. Oncoidal tufa occurs within phytoherm boundstone and the shape of the coating grains depends on the nuclei shape and prevailing environmental energy. According to Pedley (1990), highly spheroidal forms are very typical in rivers (fluvial oncoids), whereas strongly oblate spheroidal forms characterize sluggish flow regimes. Extremely spheroidal forms characterize high-energy regimes (Pentecost 2005). However, Casanova (1994) believes that environmental turbulence does not influence oncoid morphology but merely the rate of displacement.

Pisolitic tufa

Description This facies is made up of two different types of pisolitic deposits namely channel type (P) and pool type (Pp).

The first one exhibits longitudinal beds up to one meter with graded pisoid layers (Fig. 7c), whereas the pool type is mostly surrounded by boundstone facies and developed in cavities, 40–50 cm in diameter (Fig. 7d). They are composed of hard, pea-like clusters 8–12 mm in diameter somewhat similar to cave pearls. Individual pisolites are generally spheroidal or sub-spheroidal having calcite crystals or carbonate fragments of broken pisoids as nuclei.

On the other hand, elongate ones are rarely present within the channel deposits and their shapes depend on the nuclei of carbonate rock fragments. All pisolites are concentrically laminated and banded displaying well-defined boundaries and composed of micron-size broken carbonate crystals. Dark laminae have coarser anhedral and subhedral calcite crystals (approximately 10 μm) than light laminae with approximately 3–5 μm calcite crystals. Some laminae, especially pool type, contain dissolution vugs filled with chemical calcite or carbonate dusts. Outer surfaces of many pisoids were likely deformed by microboring activity. On the other hand, calcified microalgal filaments are widely present within the dark laminae of the pisolite cortex.

Interpretation Channel type pisolitic tufa is deposited in fluvial channels around the lake environment (see Fig. 7c). They display distinct depositional and crystal textures of the fluvial pisolites (e.g. Braithwaite 1979), represented by upward-graded grains with crystal cumulates formed by the mechanical breakdown and re-sedimentation of the tufa crystals. Pool type pisolites in phytoherm boundstone were precipitated in small pools. Although they generally display similar crystal texture to those of the fluvial ones (see Fig. 7d), their depositional characteristics are represented by different lithological and petrographic features. For example, lateral gradation is very distinctive for pool-type pisolite, which is characterized by increase in grain size towards the marginal part of the pool. In addition, the pisolites are always surrounded by coarse crystals growing-radial calcite crustal, established pisolite-bearing rimstone (Pentecost 2005). Although the origin of pisolitic tufa is not clearly understood, they probably may be formed by mechanical accumulation just like snowball type coating (Burgess 1983). Running and dripping-agitated waters (pool-type pisolite) would have caused accumulation of detrital carbonate grains and rolled the coats leading to pisolite growth (snowball effect). Algal filaments commonly observed in the coatings might have helped the adhesion of particles to the growing grain. Dissolution vugs within the cortex indicate the atmospheric exposures during pisolite growth intervals, and microboring on the outer coats reflect the long environmental resting after the termination of pisolite formation.

Intraclastic tufa

Description The facies is composed of homogeneous, structureless and unconsolidated silt-sand size detrital tufa fragments (see Fig. 6d). Deposits may be up to several cm in thickness and often show lenticular geometry (3–5 m wide).

Interpretation Intraclastic tufa is re-deposited within and around phytoherm framestone and within fluvial channels.

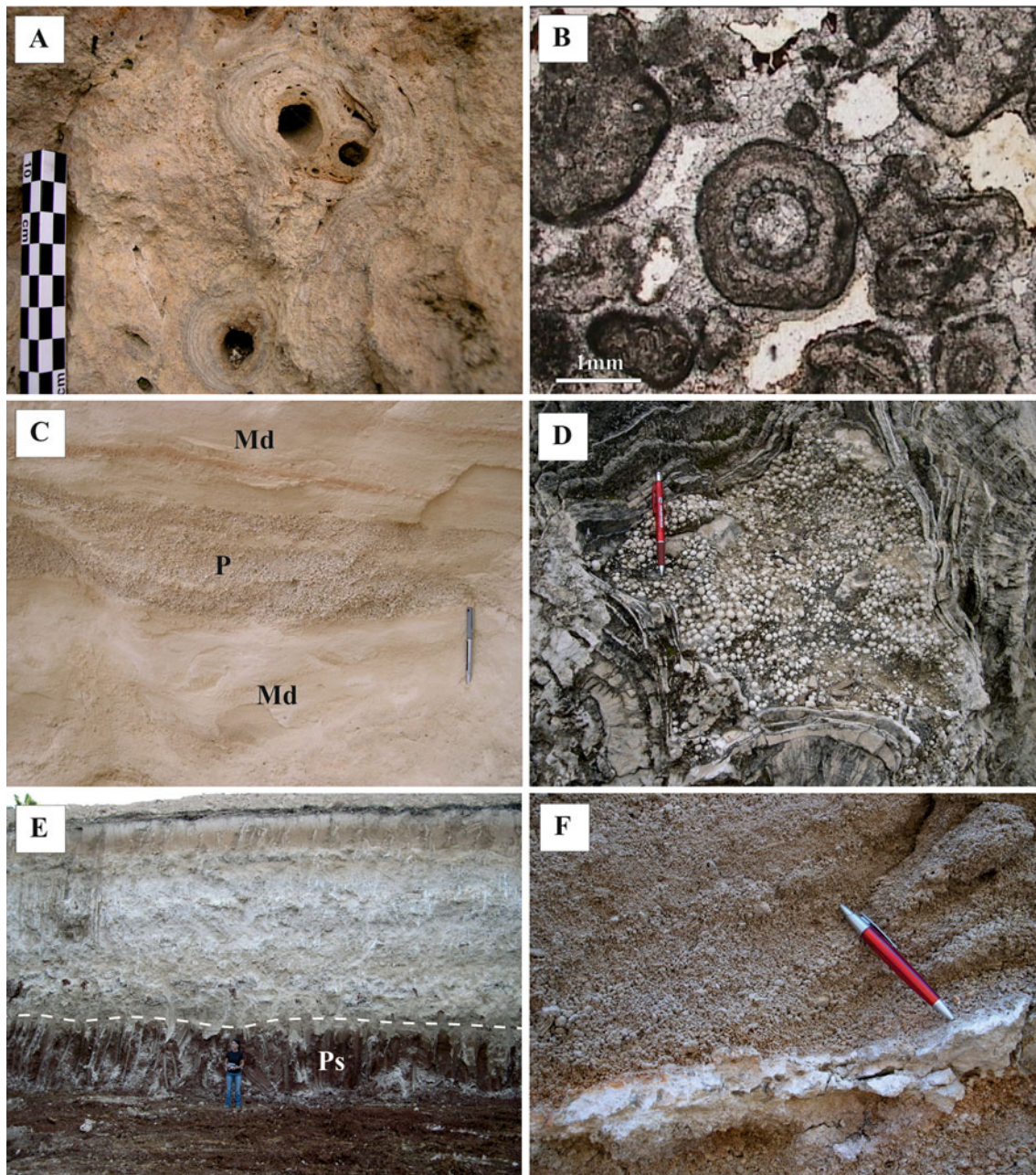


Fig. 7 Field view of oncoidal tufa facies. **a** The open spaces are calcified woods and served as nuclei during the formation of the oncoids in the weakly agitated pools, **b** Thin section of oncoidal tufa facies (104). Fresh water oncoid, nuclei formed by well-calcified macrophyte (charophyte), which likely resulted in mechanical breakdown after the death of the macrophytes under agitated water conditions. Dark and fine-grained cortex of the oncoidal grain might be directly developed by physico-chemical precipitation in the agitated small pools or the precipitation of micritic calcite during

the photosynthesis of the macrophytes and/or by the activity of microphytic epibionts; granular-blocky calcite cement around the oncoidal grains indicate the sub-water condition. Field view of **c** channel type pisolitic tufa surrounded by microdetrital tufa (Md: microdetrital tufa, P: channel type pisolitic tufa). **d** Pp: pool type pisolitic tufa. **e** Palaeosol (Ps), which is overlain by other tufa facies. **f** Cross bedded intraformational tufa conglomerate facies overlying bedded micritic tufa facies

Sediments belonging to intraclastic facies are carried by small streams flowing in the area. They have been formed by breaking up of earlier phytoherm framestone and

phytoclastic tufa facies lithologies. In addition, they also accumulate around phytoherm frameworks in static water bodies where supporting frameworks have decayed.

Microdetrital tufa

Description The facies is almost structureless and represent white coloured, very finely laminated and very fine-grained carbonates in unconsolidated zones and powdered form having 0.3–1 m thick beds. It is observed as thin mats on inclined topography, whereas it is found as thick (1–10 m) carbonate accumulations in lakes (see Fig. 7c). Lignite levels, which are 2–3 cm thick, are rarely observed in this tufa facies. The facies display lateral and vertical passages to large size detritics such as phytoclastics or pisolites.

Interpretation Although the origins of the facies are unclear, it is thought that microbial activity such as microboring may have played an important role in its formation. Several authors (e.g. Viles 1988; Pedley 1990) interpreted the facies as calcite deposition during the photosynthesis in lake and pool environments. On the other hand, pedogenic modifications related to lake level changes might have been another important factor of formation.

Palaeosols

Description The facies is made up of unconsolidated red mudstone. They contain disseminated organic materials together with fresh water gastropods and chara and root traces. It generally alternates with 1–2 cm thick phytoherm boundstone facies (see Fig. 4a). Furthermore, it is observed as a 1.5–2 m thick and laterally continuous unit along the middle and upper terrace of AT (Fig. 7e). By using the XRD determinations, they are mainly composed of quartz, calcite, multi-layered clay (chlorite + smectite), kaolinite and minor to negligible amounts of mica, hematite and feldspar in decreasing order.

Interpretation While palaeosols are one of the important indicators of the changes in the climate and tectonic regimes, tufa systems are also excellent indicators of changes in hydrologic regimes. The weathering and alteration of surrounding rocks and decomposition of organic materials are probably responsible for its formation. Golubic (1991) proposed a fluvial cycle for deposits starting in a constructional phase and finishing with an erosional retrograding phase. Related water table decrease is often indicated by pedocal soil profiles in tufa deposits.

Apart from detritic minerals such as quartz, illite and chlorite, transported to the depositional site from the surrounding areas, XRD analyses represent the presence of several diagenetic and secondary minerals (such as iron oxides and titanium oxides). It is well known that kaolinite forms from the alteration of feldspar minerals under acidic and humid climatic conditions and devitrification of

volcanic glass (Guerel and Kadir 2008). On the other hand, goethite and hematite occurrences are the results of the oxidation of iron bearing minerals within the soil.

Intraformational tufa conglomerate

Description The facies is composed of poorly sorted intraformational pebbles (0.5–10 mm in diameter) within silt to sand size detrital tufa matrix (Fig. 7f). Although most of the pebbles came from different facies described above, chert and limestone pebbles were derived from the basement rocks and made up 10 % of the facies. The majority of the pebbles are sub-rounded to rounded, unconsolidated pebbles of phytoherm framestone facies with lesser amounts of phytoherm boundstone and micritic tufa derived pebbles. Channels in the facies represent lenticular geometries with 25–30 cm thick and 2–3 m wide cross beds.

Interpretation This facies is mainly a clastic facies and developed within the fluvial channels, which is generally bounded by phytoherm boundstone and micritic tufa facies. The facies probably represents fluvial erosion of tufa, such as breaching of a tufa barrage (e.g. Pedley 1990). The fact that pebbles are well rounded to sub-rounded and in a cross-bedded structure indicates a high-energy environment.

Isotopic composition of tufa deposits and stable isotopic data

$\delta^{13}\text{C}$ and $\delta^{18}\text{O}$ isotopic values are especially sensitive indicators for the climate changes and provide important clues for determining the environmental conditions of the tufa formations (e.g. Pazdur et al. 1988; Fouke et al. 2000; Matsuoka et al. 2001). The oxygen and carbon isotopic data of AT seem to be concordant with each other (Table 3). The maximum and minimum values of $\delta^{18}\text{O}$ are -9.51 to -4.82 ‰ (PDB) and the bulk of them range between -8.39 and -5.87 ‰ (PDA) (Table 3). The carbon isotopic composition of AT displays a similar pattern to oxygen isotopes and range from -3.15 and 3.14 ‰ (PDB) and are mainly concentrated between -1.61 and 2.61 ‰ (PDB) (Table 3). The oxygen and carbon isotopic data indicate a clear linear relationship on $\delta^{18}\text{O}$ – $\delta^{13}\text{C}$ diagram (Fig. 8). But one sample distinctly displays a very low carbon isotope value (-9.42 ‰ PDB) with a higher oxygen isotope value (-4.82 ‰ PDB). $\delta^{13}\text{C}$ and $\delta^{18}\text{O}$ isotopic data of AT display diversity in the upper and middle terrace (Table 3). This diversity is more evident in the $\delta^{13}\text{C}$ data than $\delta^{18}\text{O}$ values. While the average $\delta^{13}\text{C}$ and $\delta^{18}\text{O}$ values are -6.34 and 1.94 in the upper terrace, the middle terrace

Table 3 $\delta^{13}\text{C}$ and $\delta^{18}\text{O}$ compositions for different lithotypes of the Antalya Tufa deposits shown according to their distance from the source area (the order of facies indicating moving away from the source)

Sample number	$\delta^{18}\text{O}$ (‰ VPD)	$\delta^{13}\text{C}$ (‰ VPDB)	Altitude (m)	Sample location	Lithotype
131	−6.87	2.08	317	Kızıllı (UT)	Bedded micritic tufa
116	−6.04	1.27	97	Varsak (UT)	Bedded micritic tufa
118	−5.23	3.14	170	Varsak (UT)	Stromatolitic-like tufa
119	−5.87	2.71	170	Varsak (UT)	Stromatolitic-like tufa
120	−7.32	0.60	132	Varsak (UT)	Stromatolitic-like tufa
139	−6.74	1.67	170	Varsak (UT)	Microdetrital tufa
141	−6.67	1.45	155	Varsak (UT)	Pisolitic tufa
142	−5.98	2.61	155	Varsak (UT)	Microdetrital tufa
145	−4.82	−9.42	135	Kursunlu Waterfall (MT)	Phytoherm boundstone
135	−7.74	0.03	103	Aspendos Boulevard (MT)	Intraclastic tufa
58	−9.51	−1.69	50	Çakırlar road (MT)	Phytoherm boundstone
62	−7.55	−0.91	45	Uncalı (MT)	Intraclastic tufa
64	−7.25	−0.50	35	Uncalı (MT)	Phytoclastic tufa
65	−6.63	−1.59	35	Uncalı (MT)	Intraclastic tufa
46A	−7.8	−0.82	33	Akdeniz Un. Campus (MT)	Phytoherm boundstone
46B	−8.39	−0.69	33	Akdeniz Un. Campus (MT)	Phytoherm boundstone
112	−6.5	0.42	5	Kemerağzı (MT)	Phytoherm boundstone
108	−6.53	−3.15	10	Kundu (MT)	Bedded micritic tufa

UT upper terrace, MT middle terrace

values are between -7.27 and -1.83 , respectively. Besides, $\delta^{13}\text{C}$ values of upper terrace display positive trends than middle terrace except two samples (Table 3). These isotopic differences might be due to the two cyclic periods between the upper and middle terraces.

The $\delta^{18}\text{O}$ values (-8.39 and -5.87 ‰) are nearly comparable with an equilibrium value for calcite precipitation that was derived from meteoric water (oxygen isotope composition of SMOW -7.5 ‰ at 9 °C) (e.g. Grossman and Ku 1986; Hays and Grossman 1991; Railsback 2011). Although the constant values of the $\delta^{18}\text{O}$ were only observed at the streams (e.g. Matsuoka et al. 2001), the wide range of the oxygen isotopic values of AT clearly indicates that seasonal variations of water temperatures were the most important factor in the occurrences of the tufa precipitation. In addition, local evaporation, mixing with rainwater and other non-equilibrium effects might have also played a role during the formation of the AT.

The carbon isotopes of carbonate rocks seem to be more complex than oxygen isotopes, which may have resulted from multiple potential agents (e.g. abiotic and photosynthetic) degassing of CO_2 , deposition of calcite, and CO_2 exchange with the atmosphere (Matsuoka et al. 2001). The $\delta^{13}\text{C}$ values of the AT display positive correlations with the $\delta^{18}\text{O}$ data except two samples. Two possibilities are proposed for the occurrence of the carbon isotopes in the AT. One of them may be related to the dissolution of aquifer limestone of the Mesozoic carbonates of Beydağı

allochthonous, which is represented by slightly lighter $\delta^{13}\text{C}$ values than normal marine limestones (more details in Faure 1977; Dickson and Coleman 1980). This process would be caused by equilibrium of the aquifer spring and stream water with atmospheric CO_2 (degassing) and by in-aquifer or in-stream calcite precipitation (e.g. Fouke et al. 2000; Andrews 2006).

A second possibility is photosynthesis and ventilation activity leading to preferential removal of ^{12}C and leaving the remaining HCO_3^- enriched in ^{13}C (e.g. Pitty 1971; Mertz 1992). The photosynthesis by *Chara* during summer periods extracts HCO_3^- from the lake water leading to enrichment in ^{13}C (Pitty 1971).

Matsuoka et al. (2001) indicated that the ventilation activity decreases P_{CO_2} in cave air and results in degassing of ^{12}C and causes an increase of ^{13}C . On the other hand, the ventilation process has an influence on some organism/algae and rarely corals. Similarly, phytoherm boundstone in middle terrace of AT contains microbial organism and green algae as *Shizotrix* sp., *Rivularia* sp. and *Chara* sp. (for details see Glover and Robertson 2003; Koşun et al. 2005). In addition, the $\delta^{18}\text{O}$ isotopic data of AT clearly indicate a cold-water environment. Matsuoka et al. (2001) found that cold water generally holds more CO_2 and has less potential for degassing the CO_2 than warm waters. The positive correlation trends on the $\delta^{13}\text{C}$ versus $\delta^{18}\text{O}$ diagram (Fig. 8) may be related to the winter ventilation of the cave systems, which can be one of the factors producing the

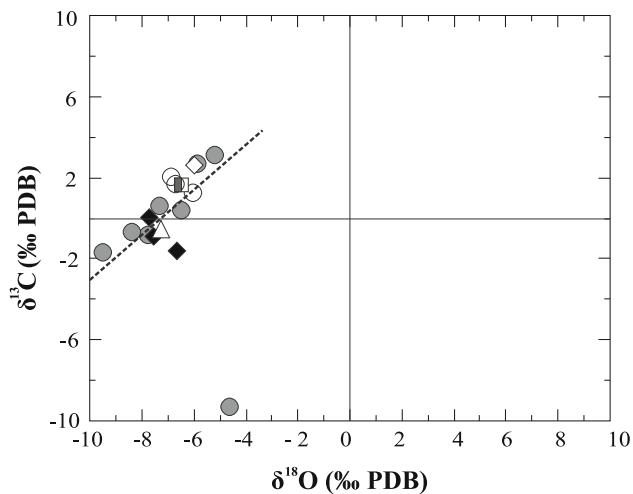


Fig. 8 $\delta^{13}\text{C}$ versus $\delta^{18}\text{O}$ diagram of different lithofacies of the Antalya Tufa. *Closed sphere* phytoherm boundstone, *closed diamond* intraclastic tufa, *closed triangle* phytoclastic tufa, *open sphere* bedded micritic tufa, *open diamond* microdetrital tufa, *half-closed square* pisolitic tufa

seasonal changes of $\delta^{13}\text{C}$ as in Shirokawa system, Japan (Matsuoka et al. 2001). The isotopically light CO_2 can be easily liberated by the decay of the organic matter in the soil, which can pull down the ^{13}C values ranging from -5 to 12 ‰ (e.g. Fouke et al. 2000). This process also seems to be suitable for AT (-3.15 and 3.14 ‰ $\delta^{13}\text{C}$, PDB), which is formed in the area of shallow groundwater and includes organic-rich interlayers and thin soil zones near the Kurşunlu area, Antalya region. The inorganic matter might have been supplied by soil water or shallow groundwater mixing with spring water near the Kurşunlu area.

Two other samples with negative carbon isotope values might be related to seasonal changes of temperatures or residence time of the spring water in the pool and terrace, which reflects partial equilibration with atmospheric CO_2 and aqueous HCO_3^- .

Although AT $\delta^{18}\text{O}$ isotopic values and depositional conditions and environments resemble to “Urrea de Jalon” defined in Ebro Basin in NE Spain (Arenas et al. 2000), a comparison with the other tufas formed in the different parts of Turkey is for the moment impossible due to the absence of published data. However, Kele et al. (2011) have recently presented new evidences of low-temperature non-equilibrium calcite-water fractionation in Pamukkale (Cotton Castle) travertines located in the Denizli Basin, Western Anatolia. Isotopic results given by the authors indicate that downstream increases of $\delta^{18}\text{O}$ travertine values are rather moderate and resultant of the superimposed isotope effects caused by carbonate precipitation, evaporation and temperature decrease.

This study additionally has pointed out that the stable isotopic data ($\delta^{18}\text{O}$, $\delta^{13}\text{C}$) of AT indicate cold-water

conditions, which are apparently affected by seasonal temperature changes (Railsback 2011). In addition, the photosynthesis with ventilation activity may have played a part in the formation of the AT deposits.

Discussion

Facies and mode of deposition

Carbonate precipitation in the travertine and tufa can be related to organic and physicochemical conditions, microbial activity, photosynthesis, water chemistry, hydrology and climatology. Although the relative importance of the processes that form tufa deposits is commonly debated, there seems to be no agreement on the issue. Many large and small tufa precipitates have characteristic deposits which depend on their sources, depositional ranges and eco-systems. It is widely accepted that cool water tufa is dominated by inorganic and organic (microphytes and macrophytes, invertebrates and bacteria) interactions (Ford and Pedley 1996; Janssen et al. 1999) and therefore can be considered to be the external sedimentary output of karstic systems (e.g. Magnin et al. 1991). A wide range of continental environments such as stream, lake, swamp and slope can be suitable for the precipitation of carbonate to form tufa. Consequently, tufa is generally considered as deposits of freshwater continental carbonate environments, widely including stromatolites, biostromes, bioherms and many coated grains (Freytet and Verrecchia 1999; Arenas et al. 2000).

The AT displays many characteristics that are common to other tufa deposits around the world (e.g. Heimann and Sass 1989; Arenas et al. 2000). According to Ford and Pedley (1996), the AT can be considered as perched springline tufa that merges into braid plain tufa. Field observations clearly indicate that fluvio-lacustrine environments are dominant in the AT, which provided suitable conditions for the deposition of microphytic and macrophytic encrustations, coated grains (pisolite and oncoid), bedded micritic tufa with non-concentric tufa stromatolitic structures and particularly detrital tufa.

Changing hydrological regimes in the springs and rapidly moving high debit water promote microbiological activity on the inclined surfaces (waterfalls, cascades) that form different kinds and shapes of microbial colonizations such as cone, dome and lateral-growth within the AT. These microbial colonizations were directly controlled by microbials depending on the spring water depth changes. *Schizothrix* sp., *Rivularia* sp. and *Scytonema* sp. contributed to the construction of these microbial structures as reported by Arenas et al. (2000). *Schizothrix* sp. displays both lateral and vertical growth positions depending on the

living environment (Freytet and Verrecchia 1999; Arenas et al. 2000). Therefore, lateral growths in phytoherm boundstone in the AT were flourished by *Schizothrix* sp. along with other microbials. On the other hand, the breakdown of these microbial communities have been the main source of formation of the micritic grains in these environments, which are directly related to the embedded bodies of *Schizothrix* sp., *Rivularia* sp. and *Scytonema* sp. in all micritic layers especially in the lake and swamp tufa. Cone and dome-shaped tufa, however, differ greatly from the former ones and belong to inner structure in the AT. They are mainly constructed of fan-shaped radial and palisadic crystals with micritic remnants and zigzag type terminations. The origins of such organic and inorganic crystals have been widely discussed by various studies (e.g. Freytet and Verrecchia 1999; Leslie et al. 1992). Freytet and Verrecchia (1999) pointed out that similar prismatic and palisadic crystals can form in early diagenetic recrystallization of micrite that can be attributed to algal build-ups of *Schizothrix* sp. Freytet and Verrecchia (1999) indicated that the filaments were contained in isometric crystals and the stems of mosses are covered by crystals arranged in a “palisadic-like fashion” (sinter crust) in oscillariace tufa. The AT is very similar to those described by Freytet and Verrecchia (1999). Specifically, micrites “microbial remnants” are very abundant within the fan-shaped masses and they are present as intercrystallines and interlayers. These micritic and organic contributions strongly suggest that the fan shaped growths are a reflection of the existence of any microbial community (likely *Schizothrix* sp.), prior to early recrystallization of the organic structures.

The present study also has similarities with the findings of Love and Chafetz (1988), who stated in their conclusion that the ‘neomorphic crusts’ formed in non-marine environments, even though devoid of organic remains, cannot be considered as inorganic deposits without detailed study. However, inorganic precipitation is a very important agent for the formation of tufa facies, due to super saturation of ambient water with respect to carbonate. In the AT, macrophytic “phytoherm framestones” facies including in situ carbonate-encrusted plant material and associated pisolitic and oncoidal facies commonly consist of inorganic encrustations, which are mostly covered by very thin algal/microbial mats. Calcified algal filaments, rod-like and microspheroidal crystals are often found within the densely packed inorganic encrustations, but they have not controlled inorganic structures, particularly pisolitic and oncoidal structures. Glover and Robertson (2003) similarly noted the importance of inorganic and organic processes in the AT facies. Spiro and Pentecost (1991) reported that the effect of photosynthesis was of minor importance and precipitation was mainly controlled by physico-chemical phenomena (temperature variation, degassing) in the tufa

environments. Some layers within the phytoclastic, intra-clastic and bedded micritic tufa facies of the AT, dominated by macrophyte-bearing facies (mostly Charophytes), heavily reflect photosynthesis that they induced carbonate sedimentation building into the thick carbonate crust. The palaeosols, which are deposited in both in upper and middle terraces, indicate that AT is formed within two cyclic periods. In the Antalya region, carbonate-rich palaeosols are often encountered as overbank deposits in fluvial environments. However, they can also be found as filling materials in phytoherm framestones and in primary tufa caves (e.g. Koşun et al. 2005). This clastic deposition was mainly controlled by seasonal changes including alternations of dry and wet periods. Additionally, a thick palaeosol development took place during a longer desiccation period of the tufa precipitation.

Apparently, the crust resulted from the precipitation of micritic calcite during the photosynthesis of the macrophytes themselves and/or by the activity of microphytic epibionts, respectively. Therefore, the process seems to be very effective on the carbonate sedimentation in the AT in which macrophytic (Charophyte) layers display strong epiphytic and internal calcification that accounts for the heavy calcification of stems (Type E) based on the classification of Schneider et al. (1983).

Age of the AT

Although there are many biostratigraphic and isotopic age data from the Antalya carbonate platform, they are inconsistent (e.g. Planhol 1956; Burger 1990; Glover and Robertson 2003).

Penck (1918) was probably one of the first researchers to mention the Antalya travertine and attribute it to the Quaternary and to the Pliocene. In previous studies (Planhol 1956; Vita-Finzi 1969; Burger 1990), Würmian (115–10 ka) (Straus 1991) and pre-Würmian ages were obtained from biostratigraphic data concerning the AT region. Isotopic ages range between 294–87 ka according to Burger (1990) and 400 to >600 ka according to Glover and Robertson (2003). These $^{230}\text{Th}/^{234}\text{U}$ isotopic ages show that the AT might have been formed from earliest >600 ka to latest 87 ka.

Biostratigraphic data

There are a few biostratigraphic studies near the Antalya and Burdur carbonate platforms (Planhol 1956). The flora, studied by Planhol (1956), led to the first biostratigraphical attribution of the AT and Burdur travertine to Würmian age (approximately 90–10 ka). Due to the presence of *Salix caprea* L. and *Salix cinerea* L. in bedded micritic facies of the middle trace, the formation of the AT would correspond to a cold climatic period of the Würmian age.

Isotopic data

Two methods have been used to date the AT.

$^{230}\text{Th}/^{234}\text{U}$ method The first isotopic study concerning the AT proposes an age range between 87 and 294 ka (Burger 1990). These pre-Würmian ages are older than the biostratigraphic ages (Planhol 1956). However, the isotopic ages of three samples, taken from the middle terrace, are within the Würmian period, which ranged from 87 to 109 ka (Burger 1990). More recently another study (Glover and Robertson 2003), based on the same method, have been applied to the AT (near Çalkaya area in middle terrace). The results are close or beyond the age limits of the Th/U method and suggest that the tufa is older than 600 ka.

In this study, two samples from the middle terrace (TU-1: Varsak region, TU-2: Konyaalti region) of the AT were collected for age dating (Table 1). Results indicate that both samples have ages around 380 ka that corresponds to a deposition at least contemporaneous to this date (Table 4).

This age discrepancy on the isotopic data might be due to contamination and/or the open system of the carbonate platform as shown in Arenas et al. (2000). Contamination and/or primitive isotopic loss could have affected the isotopic age studies.

^{14}C method In this study, ^{14}C age determinations were conducted from a lignite layer in a lake-type tufa environment situated at the upper-middle terrace escarpment base (middle terrace, near the Varsak village; see Fig. 9a, b) and from palaeosol samples in southeastern part of the middle terrace near Kemerağzı village (see Fig. 9a, c). Uncalibrated ages of these zones change from 16.85 to 3.56 ka, respectively. The relatively young C14 ages are probably because the samples came from the upper levels of lower-mid tufa terraces. Therefore, the new ^{14}C age findings indicate that the middle and lower terrace of the AT were formed contemporaneously during the Mid-Late Quaternary (Ionian-late Pleistocene) periods.

Genesis and evolution of the tufa terraces To the east of AT basin, Pliocene basement rocks are exposed (Fig. 10a). Isotopic age data indicate that the upper terrace was formed by tectonic uplift during Early-Mid Quaternary (Fig. 10b, c) (Glover and Robertson 2003; Burger 1990). Glover and Robertson's (2003) model attributes the formation of middle terrace and the submerged lower terrace to different time intervals and geological processes. Contrary to this view the model proposes a contemporaneous development of the middle and lower terraces that occurred during Mid-Late Quaternary probably including the Last Glacial Maximum (Fig. 10d, e). Following the cli-

Table 4 Th/U disequilibrium age determinations from middle terrace of the Antalya Tufa

Sample no	^{232}Th (mBq/g)	^{230}Th (mBq/g)	^{238}U (mBq/g)	^{234}U (mBq/g)	$^{230}\text{Th}(\text{aut})$ (mBq/g)	$^{234}\text{U}(\text{aut})$ (mBq/g)	$\left(\frac{^{230}\text{Th}}{^{232}\text{Th}}\right)_m$	$\left(\frac{^{234}\text{U}}{^{238}\text{U}}\right)_m$	$\left(\frac{^{230}\text{Th}}{^{234}\text{U}}\right)_m$	$\left(\frac{^{234}\text{U}}{^{232}\text{Th}}\right)_m$	$\left(\frac{^{230}\text{Th}}{^{234}\text{U}}\right)_{\text{aut}}$	$^{230}\text{Th}/^{234}\text{U}$ age (years)	Error on age (years) (in years, uncertainties: 2σ , i.e. 95 % confidence interval)
TU-1	1.43	4.71	4.29	4.52	3.28	3.09	3.29	1.06	3.16	1.062	1.062	>380.000	–
TU-6	0.41	5.28	4.75	4.95	4.88	4.54	13.02	1.04	12.21	1.073	1.073	>380.000	–

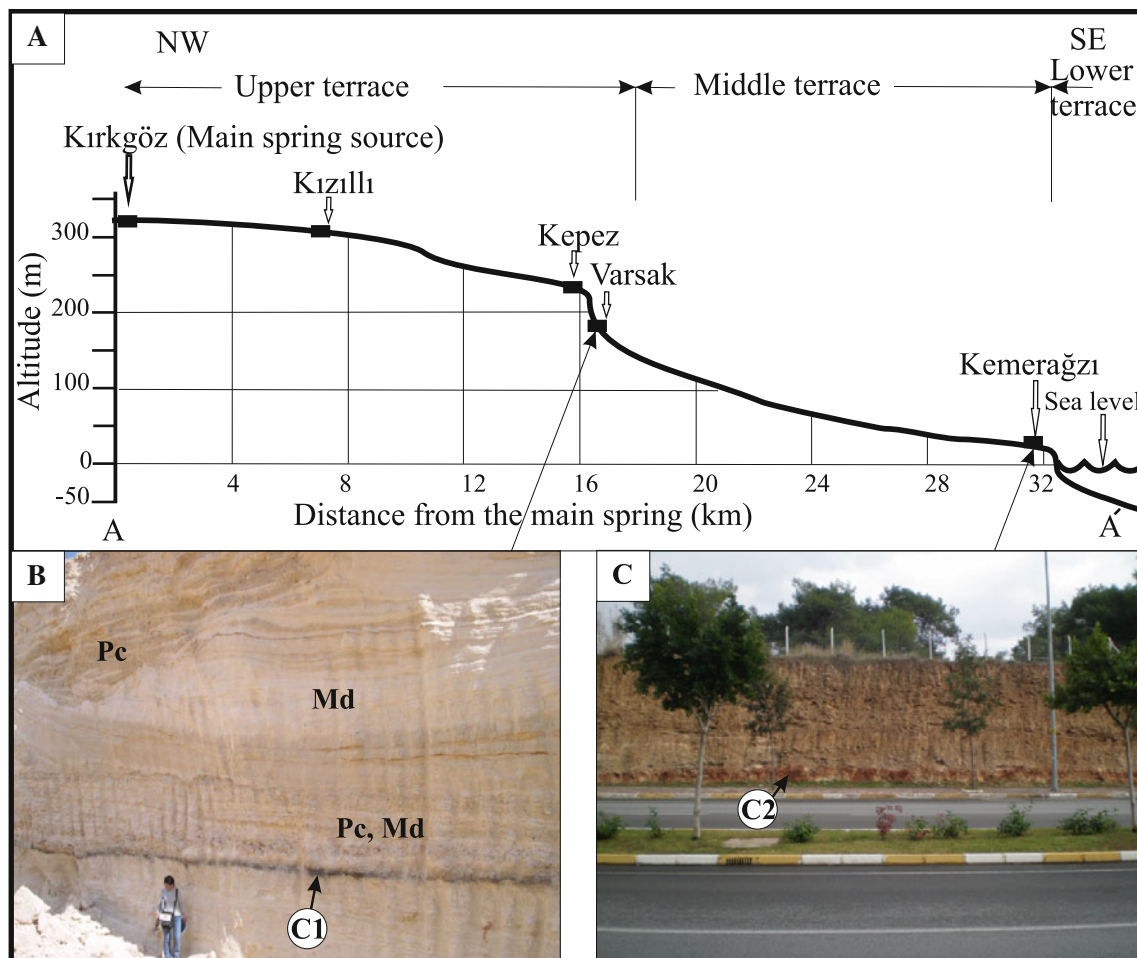


Fig. 9 a Topographic profile of the Antalya tufa deposits, b lake-type tufa facies of the upper terrace near Varsak village, (Pc: phytoclastic, Md: microdetrital), c tufa facies of the middle terrace in SE of

Kemeragzi village (palaeosols, phytoherm framestone, phytoherm boundstone). C1: ^{14}C age sample zone of the lignite, C2: ^{14}C age sample zone of palaeosols

matic changes that occurred in Holocene the lower terrace was submerged to its present position (Fig. 10f). Probable tectonic local uplift and coastal cliff erosion is at the origin of the formation of the third escarpment at the middle terrace (Fig. 10g). According to Desruelles et al. (2009) and Çiner et al. (2009) major causes of sea level changes observed along the Turkish Mediterranean coast during the last 3,000 years can be attributed to local tectonics rather than to climate and/or glacio-eustasy.

In the proposed terrace evolution model, the middle and lower terraces of AT were clearly formed together during the Mid-Late Quaternary (Ionian-late Pleistocene) periods. On the contrary, in the model of Glover and Robertson (2003) the transgression was developed after the second terrace formation during the Early-Mid Quaternary. If the transgression was developed after the second (middle) terrace in that time interval, mentioned by Glover and Robertson (2003), marine sedimentation should have accompanied the upper surface of the second terrace. However, there was no data noted concerning marine

sedimentation (transgression) or erosion surfaces on the upper surface of the second terrace.

Conclusion

Field observations, stratigraphic studies, $\delta^{13}\text{C}$ and $\delta^{18}\text{O}$ isotopic values and ^{14}C age studies of the AT indicate the following results:

- AT is classified into two sub-groups as autochthonous (boundstone, phytoherm framestone, bedded micritic tufa) and allochthonous tufa facies (phytoclastic tufa, oncoidal tufa, pisolitic tufa, intraclastic tufa, microdetrital tufa, palaeosols and intraformational tufa conglomerate) that have been deposited in fluvial, paludal, lacustrine and waterfall-cascade environments. The boundstone facies of the allochthonous sub-group is divided into two new sub-facies according to their origin as “phytoherm boundstone” and “stromatolitic-

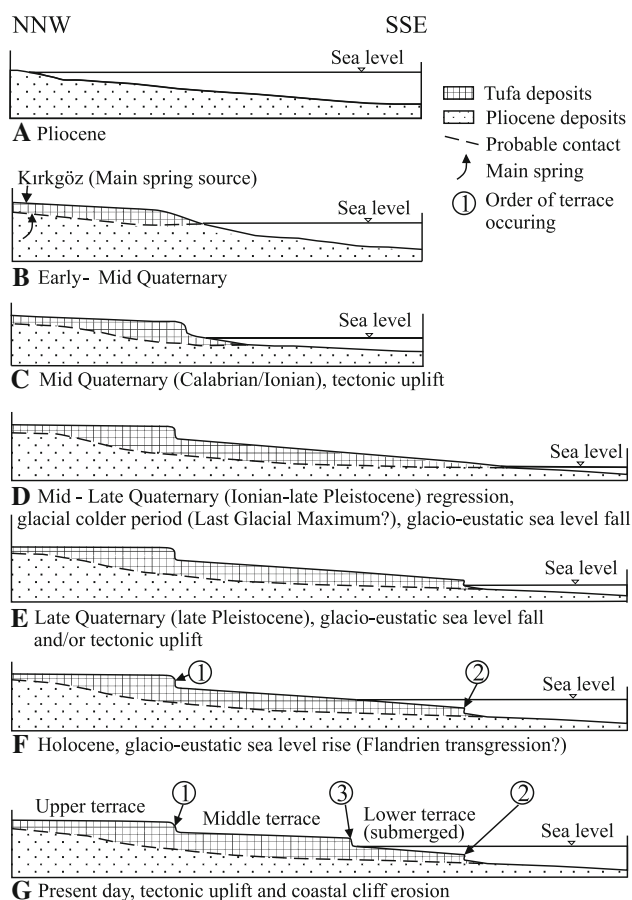


Fig. 10 Hypothetical depositional evolution model of the terrace morphology of Antalya Tufa

like tufa". Pisolitic tufa of allochthonous tufa facies is composed of two new facies as pool-type and channel-type. AT represents a typical example of terraced cool-water modern carbonate-precipitation system.

- The $\delta^{18}\text{O}$ and $\delta^{13}\text{C}$ values of AT clearly display cold-water conditions in the genesis of the tufa deposits. The minor isotopic differences between upper and middle terrace and 1.5–2 m. Palaeosol levels at the upper and middle terrace may have resulted from two cyclic periods in formation of the terrace of AT.
- The upper terrace deposition occurred during Early-Mid Quaternary by tectonic uplift. Following the deposition, the first escarpment was probably formed in Mid Quaternary. Lower and middle terrace depositions are both controlled by eustatic sea level changes and tectonic uplift that occurred during Mid-Late Quaternary. The formation of the second escarpment at the lower terrace (Latest Pleistocene-Holocene) by glacio-eustatic sea level rise is followed by the formation of the third escarpment in the middle terrace (Holocene to Recent) by tectonic uplift and coastal cliff erosion.

- The $^{230}\text{Th}/^{234}\text{U}$ ages obtained from the lower parts of the middle terrace indicate that the deposition started at least prior to 380 ka. The ^{14}C ages (16.85 and 3.56 ka) obtained from the upper parts of the middle terrace indicate that the deposition lasted till at least 3.56 ka.

Acknowledgments Financial support for this study was provided by Akdeniz University Scientific Research Project. I would like to thank Baki Varol (Ankara University, Turkey), Erkan Aydar (Hacettepe University, Turkey) and Olivier Monod (Orléans University, France) for the field and SEM studies. The author acknowledges the comments of Attila Çiner (Hacettepe University, Turkey), André Poisson (Orsay University, France), M. Cemal Göncüoğlu (Middle East Technical University, Turkey) and Semih Gürsu (MTA, Turkey), who reviewed an earlier version of this paper. I would like to thank Muhammet Satır (Tübingen University, Germany) and Uğur Temiz (Bozok University, Turkey) for the isotopic analyses and Sandor Kele (Hungarian Academy for sciences, Budapest) for the interpretation of isotopic analyses results and Marc Massault (Université Paris 11, France) for the analyses of radiogenetic carbon dating. I also appreciate careful comments of the anonymous reviewers that improved the quality of the manuscript.

References

- Altunel E (1996) Morphologic characteristics, age and neotectonics importance of Pamukkale Travertines. *Miner Res Explor Bull (Ankara)* 118:47–64 (In Turkish)
- Andrews JE (2006) Palaeoclimatic records from stable isotopes in riverine tufa: synthesis and review. *Earth Sci Rev* 75:85–104
- Arenas C, Gutierrez F, Osácar C, Sancho C (2000) Sedimentology and geochemistry of fluvio-lacustrine tufas deposits controlled by evaporite solution subsidence in the central Ebro Depression, NE Spain. *Sedimentology* 47:883–909
- Arp G, Hofmann J, Reitner J (1998) Microbial fabric formation in spring mounds ("Microbialites") of alkaline salt lakes in the Badain Jaran Sand Sea, PR China. *Palaio* 13(6):581–592
- Braithwaite CJR (1979) Crystal textures of recent fluvial pisoliths and laminated crystalline crusts in Dyfed, South Wales. *J Sediment Pet* 49:181–194
- Burger D (1990) The travertine complex of Antalya, southwest Turkey. *Zeitschrift für Geomorphologie* 77:25–46
- Burges CJ (1983) Quaternary pisoids of Lau, Fiji. In: Peryt TM (ed) *Coated grains*, pp 488–502
- Carthew KD, Taylor MP, Drysdale RN (2006) An environmental model of the fluvial tufas of the seasonally humid tropics, northern Australia. *Geomorphology* 73:78–100
- Casanova J (1994) Stromatolites from the East African Rift: a synopsis. In: Bertrand-Sarfati J, Monty CLV (eds) *Phanerozoic stromatolites II*, pp 193–226
- Chafetz HS, Lawrence JR (1994) Stable isotopic variability within modern travertines. *Geographie Physique et Quaternaire* 48(3):257–273
- Çiner A, Karabiyiçoğlu M, Monod O, Deynoux M, Tuzcu S (2008) Late Cenozoic sedimentary evolution of the Antalya Basin, Southern Turkey. *Turk J Earth Sci* 17:1–41
- Çiner A, Desruelles S, Fouache E, Koşun E, Dalongeville R (2009) Beachrock formations on the Mediterranean Coast of Turkey: implications for Holocene sea level changes and tectonics. *Geol Bull Turk* 52(3):257–297
- Desruelles S, Fouache É, Çiner A, Koşun E, Dalongeville R, Pavlopoulos K, Coquinot Y, Potdevin JL (2009) Beachrocks and

- sea-level changes since Mid-Holocene: comparison between the insular group of Mykonos-Delos-Rhenia (Cyclades, Greece) and the southern coast of Turkey. *Glob Planet Change* 66:19–33
- Dickson JAD, Coleman ML (1980) Changes in carbon and oxygen isotope composition during limestone diagenesis. *Sedimentology* 27:107–118
- Ekmekci M (2005) Pesticide and nutrient contamination in the Kestel polje-Kirkgoz karst springs. *South Turk Environ Geol* 49(1):19–29
- Faure G (1977) *Isotope geology*. Wiley, New York, p 464
- Flecker R, Poisson A, Robertson AHF (2005) Facies and palaeogeographic evidence for the Miocene evolution of the Isparta Angle in its regional Eastern Mediterranean context. In: Kelling G, Robertson AHF, van Buchem F (eds) *Cenozoic sedimentary basins of South Central Turkey*. *sedimentary geology*, vol 173, pp 277–314
- Ford TD, Pedley HM (1996) A review of tufas and travertines deposits of the world. *Earth Sci Rev* 41:117–175
- Fouke BW, Farmer JD, Des Marais DJ, Pratt L, Sturchio NC, Burns PC, Discipulo MK (2000) Depositional facies and aqueous-solid geochemistry of travertine-depositing hot spring (Angel Terrace, Mammoth Hot Springs, Yellowstone National Park, USA). *J Sediment Res* 70(3):565–585
- Freytet P, Verrecchia EP (1999) Calcitic radial palisadic fabric in freshwater stromatolites: diagenetic and recrystallized feature or physicochemical sinter crust? *Sed Geol* 126:97–102
- Glover C, Robertson AH (2003) Origin of tufas (cool-water carbonate) and related terraces in the Antalya areas, SW Turkey. *Geol J* 38:1–30
- Golubic S (1991) Modern stromatolites—a review. In: Riding R (ed) *Calcareous algae and stromatolites*. Springer-Verlag, Berlin, pp 541–561
- Gonzalez LA, Carpenter SJ, Lohman KC (1992) Inorganic calcite morphology: roles of fluid chemistry and fluid flow. *J Sediment Petrol* 62:382–399
- Grossman EL, Ku TL (1986) Oxygen and carbon isotope fractionation in biogenic aragonite—temperature effects. *Chem Geol* 59(1):59–74
- Guerel A, Kadir S (2008) Geology and mineralogy of Late Miocene clayey sediments in the southeastern part of the Central Anatolian Volcanic Province, Turkey. *Clays Clay Miner* 56(3):307–321
- Guo L, Riding R (1998) Hot-spring travertine facies and sequences, Late Pleistocene, Rapolano Terme, Italy. *Sedimentology* 45:163–180
- Hays PD, Grossman EL (1991) Oxygen isotopes in meteoric calcite cement as indicators of continental palaeoclimate. *Geology* 19:441–444
- Heimann A, Sass E (1989) Travertines in the Northern Hula Valley, Israel. *Sedimentology* 36:95–108
- Janssen A, Swennen R, Podoor N, Keppens E (1999) Biological and diagenetic influence in recent and fossil tufa deposits from Belgium. *Sed Geol* 126(1–4):75–95
- Jones B, Renaut RW, Rosen MR (2000) Trigonal dendritic calcite crystals forming from hot spring waters at Waikite, North Island, New Zealand. *J Sediment Res* 70:586–603
- Kele S, Özkul M, Forizs I, Gökğöz A, Baykara MO, Alçiçek MC, Tibor Nemeth T (2011) Stable isotope geochemical study of Pamukkale travertines: new evidences of low-temperature non-equilibrium calcite-water fractionation. *Sed Geol* 238(1–2):191–212
- Koşun E, Sarıgül A, Varol B (2005) Lithofacies characteristics of Antalya Tufa. *Min Res Explor Bull (Ankara)* 130:57–70 (In Turkish)
- Leslie AB, Tucker ME, Spiro B (1992) A sedimentological and stable isotopic study of travertines and associated sediments within Upper Triassic lacustrine limestones, South Wales, UK. *Sedimentology* 39(4):613–631
- Love KM, Chafetz HS (1988) Diagenesis of laminated travertine crusts, Arbuckle Mountains, Oklahoma. *J Sediment Petrol* 58(3):441–445
- Magnin F, Guendon JL, Vaudour J, Martin P (1991) Les travertins: accumulations carbonatées associées aux systèmes karstiques, séquences sédimentaires et paléoenvironnements Quaternaires. *Bulletin de la Société Géologique de France* 162:585–594
- Matsuoka J, Kano A, Oba T, Watanabe T, Sakai S, Seto K (2001) Seasonal variation of stable isotopic compositions recorded in a laminated tufa, SW Japan. *Earth Planet Sci Lett* 192:31–44
- McCrea JM (1950) On the isotopic chemistry of carbonates and a paleotemperature scale. *J Chem Phys* 18:849–857
- Mertz M (1992) The biology of carbonate precipitation by cyanobacteria. *Facies* 26:81–102
- Özkul M, Varol B, Alçiçek MC (2003) Petrographic characteristics and depositional environments of Denizli Travertines. *Miner Res Explor Bull* 125:13–29 (In Turkish)
- Özüş S (1992) Antalya travertines, hydrology and geochemistry. Unpublished PhD thesis, University of Çukurova, Adana, Turkey (In Turkish)
- Pazdur A, Pazdur MF, Starkel L, Szulc J (1988) Stable isotopes of Holocene calcareous tufa in Southern Poland as paleoclimatic indicators. *Quatern Res* 30:177–189
- Pedley HM (1990) Classification and environmental models of cool freshwater tufas. *Sed Geol* 68:143–154
- Pedley M (2009) Tufas and travertines of the Mediterranean region: a testing ground for freshwater carbonate concepts and developments. *Sedimentology* 56(1):221–246
- Penck N (1918) *Die tektonischen Grundzüge westkleinasiens*: Engelhorn Nachf., Stuttgart
- Pentecost A (2005) *Travertine*. Springer-Verlag, Berlin
- Pitty AF (1971) Rate of uptake of calcium-carbonate in underground karst water. *Geol Mag* 108(6):537–543
- Planhol XD (1956) Contribution à l'étude géomorphologique de Taurus occidental et de plaines bordières. *Revue de Géographie Alpine* 44:609–685
- Poisson A, Wernli R, Sagular EK, Temiz H (2003) New data concerning the age of the Aksu Thrust in the south of the Aksu Valley, Isparta Angle (SW Turkey): consequences for the Antalya Basin and the eastern Mediterranean. *Geol J* 38:311–327
- Railsback LB (2011) Some fundamentals of mineralogy and geochemistry. <http://www.gly.uga.edu/railsback/FundamentalsIndex.html#Isotopes>
- Sant'Anna LG, Riccomini C, Rodrigues-Francisco BH, Sial AN, Carvalho MD, Moura CAV (2004) The Paleocene travertine system of the Itaboraí basin, Southeastern Brazil. *J S Am Earth Sci* 18:11–25
- Schneider S, Schroder HG, Le Campion-Alsumard T (1983) Algal micro-reefs, coated grains from freshwater environments. In: Peryt TM (ed), *Coated grains*. Springer-Verlag, Berlin, pp 284–298
- Şenel M (1997) Geological map series of Turkey 1:100 000 scale, Antalya L 11 sheet. Publications of Mineral Research and Exploration, Ankara
- Spiro B, Pentecost A (1991) One day in the life of a stream- a diurnal inorganic carbon mass balance for a travertine-depositing stream (Waterfall beck, Yorkshire). *Geomicrobiol J* 9(1):1–11
- Straus LG (1991) Southwestern Europe at the last glacial maximum. *Curr Anthropol* 32(2):189–199
- Viles HA (1988) *Biogeomorphology*. Basil Blackwell, Oxford
- Vita-Finzi C (1969) Late quaternary continental deposits of Central and Western Turkey. *Man New Ser* 4(4):605–619